Submitted to: 42nd National Symposium American Vacuum Society
Minneapolis, MN October16-20, 1995

BNL-62540
CONF-951030--6

Paper submitted to JVST - AVS proceedings. Oct. 1995

New Developments in IR Surface Vibrational Spectroscopy

C.J. Hirschmugl[†], C.L.A. Lamont[‡] and G. P. Williams

National Synchrotron Light Source

Brookhaven National Laboratory

Upton, NY 11973-5000

Abstract

Low frequency dynamics at surfaces, particularly in the region of the adsorbate-substrate vibrational modes is of fundamental importance in areas as varied as sliding friction, catalysis, corrosion and epitaxial growth. This paper reviews the new developments in low frequency Infrared Reflection Absorption Spectroscopy using synchrotron radiation as the source. Absolute changes induced in the far infrared for several adsorbate systems on Cu, including CO and H, are dominated by broadband reflectance changes and dipole forbidden vibrational modes which in some cases are an order of magnitude stronger than the dipole allowed modes. The experimental data can be explained by a theory developed by Persson, in which the dielectric response of the substrate is seen as playing a crucial role in the dynamics. In particular the relationships between the wavelength of the light, the penetration depth and the electron mean-free path, are critical.

*Work performed under the auspices of the U.S. Department of Energy, under contract DE-AC02-76CH00016

1. Introduction

Surface vibrational spectrocopy has developed in two areas in the past 5 years. On the first front, High Resolution Electron Energy Loss Spectroscopy (HREELS), which has the capability of studying low frequency modes down to a few meV, or a few 10's of wave-numbers (cm^{-1}), has been improving in resolution[1]. The latest instruments have a resolution of 1 meV or even better and with good counting rates. On the second front, Infrared Reflection Absorption Spectroscopy (IRAS), which has an intrinsically higher resolution of 100 μev or better, has been developed to lower frequencies using synchrotron radiation as a source[2,3]. With its 1000-fold improvement in brightness over thermal sources, higher stability and absolute output, this has enabled absolute reflectivity changes to be measured to 0.2% with a reproducibility of .02% in acquisition times of 1 minute down to 50 cm^{-1} and with 1 cm^{-1} resolution.

In this paper we report on the development and results obtained using the synchrotron source for various sub-monolayer adsorbate systems on single crystal Cu substrates and show how many unexpected phenomena that have been observed can be explained in terms of a relatively simple physical picture.

2. Experimental Procedures.

All the experiments were perfomed at beamline U4IR at the National Synchrotron Light Source. The white beam was focused through either a diamond or CsI window, collimated and passed into a Nicolet Impact 410 rapid-scan Michelson interferometer. Si was used as a beamsplitter. The beam emerging from the interferometer was focused at f/10 onto the sample in the center of an ultra-high vacuum chamber of diameter 300mm. The angle of incidence was 87°. Simultaneous dosing, LEED, IRAS and TPD spectroscopy can be performed in this chamber. The reflected beam was focused into the Winston cone of a liquid helium cooled (4.2K) boron doped Si bolometer for the low frequency measurements (50 - 500 cm^{-1}) or onto the element of a Cu doped Ge photoconductive detector, also at 4.2K, for the higher frequency measurements (350 - 2500 cm^{-1}). An important feature of using synchrotron radiation is that the signal is strictly proportional to the beam current in the electron storage ring, assuming a stable orbit, enabling absolute reflectivity measurements to be made[4]. This was checked by repeating measurements for a clean crystal, and normalizing to the beam current. It was found that reproducibilities of ±0.2% could reliably be obtained over periods of 20 minutes with stored but decaying beam in the storage ring. If the beam current was maintained by frequent injections every few minutes, then the ±0.2% reproducibility could be maintained over much longer periods. We evaluated this for periods in excess of an hour and attribute the results to

better thermal stability of the synchrotron storage ring when operated at constant current. This will be important in future measurements.

The Cu single crystal samples used for these experiments had faces of dimensions 25mm x 6mm and they were mechanically polished, then electropolished before being inroduced into UHV. Details of this preparation are given in Ref. 5. Prior to the IRAS experiments, the samples were sputtered with Ne^+ at 1x10-4 Torr, at 500 eV and 300 K for 20 minutes at grazing incidence (from both directions). The samples were then briefly annealed to 850 K and showed very sharp LEED spots. Auger spectra showed no sulfur, carbon or oxygen or other impurities to a limit of <2% of the Cu (105 eV) peak.

The IRAS measurements were all made by first taking several sets of scans on the clean surface and verifying the reproducibility. Then the sample was dosed and re-measured. The CO dosing was done by back-filling the UHV chamber with CO gas with the sample at 90K. The H dosing was done with the sample at 140K to eliminate co-adsorption of water. The H_2 gas was introduced into the chamber via a dosing tube which was terminated in a W coil at 1500K. A LEED pattern corresponding to a (3x3) pattern of H on the surface was obtained after dosing with the chamber background pressure at $2x10^{-7}$ for ~ 5 minutes. In all the data presented here, only the *changes* in the reflectivity, induced by the adsorbate, are shown.

3. Results and Discussion.

In Fig. 1 we show the reflectivity changes induced by the adsorption of CO on Cu(100), (111) and (110). In addition to the expected dips in the spectrum due to the internal carbon-oxygen vibration at ~ 2100 cm^{-1} and the carbon-metal vibration at ~ 340 cm^{-1}, a broadband frequency dependent change is observed as well as a peak at ~ 275 cm^{-1}. Double isotopic substitution of the CO confirmed that this peak is consistent with the dipole forbidden frustrated rotation mode[6]. Note that the carbon-metal mode is about 2 orders of magnitude weaker than the internal C-O stretch mode.

In Fig. 2 we show reflectivity changes induced on a Cu(111) surface by a (3x3) H overlayer. A broadband background change is observed as for CO, with a peak at 770 cm^{-1}. Experiments on D were performed[7] and showed an isotopic shift of this peak to 590 cm-1, consistent with it being a parallel vibrational mode - the frustrated translation.

For infrared radiation incident at near grazing incidence on a metal surface[8], the parallel field is lower than the perpendicular field by the ratio ω/ω_p where ω_p is ~ 10^5 cm^{-1}. At 1000 cm^{-1} the parallel electric field intensity is thus 10^{-2} and the intensity 10^{-4} of the perpendicular field, which is the basis of the so called dipole selection rule. Due

to the continuity of the electric field at the surface, however there will also be a parallel field of the same magnitude below the surface. For EELS the situation is different since the parallel field is suppressed due to screening of the incoming electronic charge, and is 10^{-4} times the perpendicular field. The intensity is therefore down by a factor of 10^{-8}, see Fig. 3.

Although for IR measurements the parallel field is weaker at a metal surface, if we examine the relationship between the penetration depth, mean-free-path and frequency of the incoming light in the vicinity of the surface of a metal such as Cu[9], and illustrated in Fig. 4, we see that the surface plays an important role in the electron scattering and hence absorption dynamics. For the experiments reported here we are either in region D, the anomalous skin effect region, at low frequencies, or region E, the extreme anomalous skin effect region at the higher frequencies. In both cases, the mean-free-path is longer than the penetration depth of the light and the surface is the predominant scattering site. One might therefore expect the presence of adsorbates to modify the IR reflectivity. It is also important to note that at low frequencies the electric field experienced by the electrons in the substrate varies appreciably over a distance compared with the mean free path, i.e. the induced current is not related to the field by the relationship $\mathbf{J}^{ind}=\sigma\mathbf{E}$ and the local optics approximation breaks down.

Using these concepts, Persson[10-14] has calculated the response of a surface to the changes induced by the addition of adsorbates as scattering centers. If we take a

simple picture of an adsorbate, such as a H atom, on a surface, then we can write an equation of motion for the parallel displacement **u** of the adsorbed atom thus:

$$\ddot{\mathbf{u}} + \omega_o^2 \mathbf{u} + \eta(\dot{\mathbf{u}} - \mathbf{v}) + \gamma \dot{\mathbf{u}} = 0 \qquad (1)$$

where **v** is the parallel drift velocity of the conduction electrons at the surface, induced by the external electric field **E** of the incoming light beam and ω_o is the resonance frequency of the frustrated translation. In this expression there is a friction force $\mathbf{f}_1 = -M\eta(\dot{\mathbf{u}} - \mathbf{v})$ which depends on the relative velocity between the adsorbate (mass M) and the drift velocity **v** and is similar to the force which acts on a body in streaming water, which, of course, depends only on the *relative* velocity between the body and the water. There is also an additional force $\mathbf{f}_2 = -M\gamma\dot{\mathbf{u}}$ due to damping via multi-phonon emission. For H on Cu this term is negligible but the damping could still occur due to lateral tunneling of the adsorbates and to dephasing processes. The time-averaged adsorbate induced power absorption is:

$$P = -n_a A(\langle \mathbf{f}_1 \cdot (\dot{\mathbf{u}} - \mathbf{v}) \rangle + \langle \mathbf{f}_2 \cdot \dot{\mathbf{u}} \rangle) \qquad (2)$$

where A is the surface area and n_a the concentration of adsorbates. P can be calculated to linear order in n_a by using the drift velocity **v** obtained without adsorbates. The change in the IR reflectivity induced by the adsorbates is given by $\Delta R = -P/I_0 A_0$ where A_0 is the cross-sectional area of the incident photon beam. If the angle of incidence is θ, the surface area A covered by the incident beam is $A = A_0/\cos(\theta)$. The intensity of the incident IR beam is determined by the Poynting

vector and is given by $I_0 = cE_0^2/8\pi$, where E_0 is the amplitude of the electric field of the incident light beam. Combining these relationships with the Fresnel formula for the electric field in the metal and taking account of non-local optics, gives:

$$\Delta R = -\frac{4}{c}\frac{n_a}{n}\frac{M}{m}\frac{\eta}{\cos\theta}\left(1-\frac{\omega^2\eta(\eta+\gamma)}{\left(\omega^2-\omega_o^2\right)^2+\omega^2(\eta+\gamma)^2}\right)\frac{\omega^2}{\omega^2+\frac{6}{5}b^2} \qquad (3)$$

where b is equal to the Fermi velocity divided by the skin depth, $v_F/\delta = 440\ cm^{-1}$, for Cu. This formula predicts a broadband background change, and an enhanced reflectivity at the frequency of the frustrated translation, $\omega = \omega_0$ yielding an anti-absorption peak of width $\Gamma = \eta + \gamma$ and whose area is independent of γ.

It is important to note that Tobin has shown that the broadband frequency response of a metal can be related to the change in DC resistivity independently of the relaxation time of the adsorbate parallel mode[15].

The simplest application of Eq. 3 is to an atom such as hydrogen on the surface. In Fig. 2 the solid line represents a fit to the background change. The discrepancy at high frequencies is attributed to induced electronic states at the surface. Considering now the anti-absorption peak due to the dipole forbidden frustrated translation mode, and using the second term of Eq. 3 which is related to the peak as shown in the inset to Fig. 2, the linewidth of the anti-absorption peak is $\Gamma \approx 62\ cm^{-1}$ and $\eta/(\gamma+\eta) \approx 0.12$. Hence, $\eta \approx 7.5\ cm^{-1}$ and $\gamma \approx 54.5\ cm^{-1}$. An electronic friction $\eta \approx 7.5\ cm^{-1}$ corresponds to a lifetime $\tau = 0.7\ ps$. One can also determine η from the high frequency value of

the background absorption, given by the high frequency limit of the last term in Eq. 3 multiplied by the first term. Using a value of $n_a = 0.124\ \mathring{A}^{-2}$, corresponding to a coverage $\theta = 0.7$ which has been suggested for the (3×3)H overlayer we obtain $\tau \approx 3$ *ps* or $\eta \approx 1.7\ cm^{-1}$. This value for τ is about a factor of 4 larger than that deduced from the area under the anti-absorption peak, a discrepancy which is understood in terms of the background absorption being due to collective motions for which there will be a contribution from interference between the electron probability amplitude waves scattered from different adsorbates along the surface. A similar effect was found for thin-film resistivity measurements for H on Ni(111)[16], where the adsorbate induced contribution to the film resistivity (per adsorbate) was a factor of 4 smaller at high coverages.

It is possible to apply the same physical arguments to the case of a molecule such as CO[17]. The fits to the background are shown in Fig.1 and very good agreement is obtained. When considering the anti-absorption feature similar arguments can also be applied, although here since the frustrated rotation is not a purely parallel mode, a modified value of η has to be used. The results of a fit to the anti-absorption are shown in Fig. 5. Very good agreement is obtained even though there are no fitting parameters, and the damping derived from the analysis corresponds to e-h pair lifetimes of 3 and 1 picoseconds for the (100) and (111) surfaces respectively, which are reasonable values.

4. Chemical shifts and intermolecular coupling.

Thus far we have discussed effects which are a consequence of interactions between the substrate and the overlayer. In addition to this, there are intermolecular effects from dipole-dipole and other coupling mechanisms. These effects are revealed by coverage dependent shifts in mode frequencies, but are complicated by concomitant chemical shifts, which themselves are interesting since they may yield information about the bonding. In principle for dipoles perpendicular to the surface, coupling interactions stiffen the coupled vibrational modes. For parallel modes both end-to-end softening terms as well as side-by-side stiffening terms compete in determining what happens but for most of the surface meshes a softening is expected[18]. Measurements of these effects provides considerable insight into the surface dynamics and they have been studied for intramolecular modes. Such studies of intramolecular modes can only indirectly probe the bond at the surface whereas the present study extended this work directly to the modes closely associated with the bonding.

To separate chemical from coupling effects it is necessary to use mixtures of isotopes[19]. If one measures the difference in frequency between the value of a mode in the dilute coverage (dilution) limit and that for a higher coverage, both chemical and coupling effects will have played a role in determining the final frequency. If, however the molecule is studied first at low coverages, then at high coverages but surrounded by molecules of a different isotopic, but similar chemical, composition, any observed

differences will have exclusively a chemical origin. The difference between the frequencies observed for the dilution limit and the homogeneous limit indicate the strength of the coupling.

In Fig. 6 we show a series of spectra taken for a Cu(100) surface for a coverage of 0.25 monolayers, and a set of isotopic mixtures at a total coverage of 0.5 monolayers. The anti-absorption feature from the frustrated rotation, and the carbon-metal modes are clearly visible as doublets for the isotopic mixtures with an adequate signal to noise to enable the coupling and chemical shifts to be extracted as shown in Fig. 7. If dipole-dipole coupling predominates, as is the case for the C-O stretch, then the interactions can be understood in terms of a theory[20] which includes an approach to treating the disorder in the isotopic mixtures via the coherent potential approximation (CPA) used in the calculation of the electronic structure of alloys. Given the homogeneous and dilute limit frequencies for both isotopes and the isotopic mixture, this theory predicts both the frequency shifts and the strengths as a function of composition for the isotopic mixtures with no adjustable parameters. Using this formalism, we obtain the results shown as the dotted lines in Fig. 6. Note that no background slope was included in this theory, whereas the peaks in this region are on a small background slope. The agreement for the shifts and the intensities, including the effects of intensity borrowing, is remarkable.

From these shifts and also from the integrated intensities, one can determine the vibrational polarizabilities[21]. Thus for the carbon-metal stretch mode the polarizability

is 0.038 $Å^3$ as determined from peak positions assuming dipole-dipole coupling, and 0.022 $Å^3$ from integrated intensity measurements. This compares with a value of 0.25 $Å^3$ for the internal stretch mode. For the parallel modes the intensities are not determined by the dynamic dipole moment and such a comparison cannot be made.

5. Summary.

We have shown how studies of the low frequency response of adsorbate covered Cu surfaces give insight into new dynamical processes. Unexpected broadband reflectance changes and the appearance of dipole-forbidden modes as anti-resonances in the reflectance spectra can be explained both qualitatively and qunatitatively in terms of a relatively simple model. Mixed isotope experiments allow both chemical and coupling effects to be studied for the bonding vibrational modes yielding insight into mechanisms important to the understanding of sticking, friction and dynamics.

Acknowledgements.

We are extremely grateful for the technical support of G. Nintzel, D. Carlson and T. Lenhard and the NSLS support staff and for discussions with F. Hoffmann and P. Dumas. We are extremely grateful to B. Persson both for continued discussions and

for providing detailed assistance with the CPA calculations. CLAL ackowledges a travel grant from the U.K. Science and Engineering Research Council. The NSLS is supported by the United States Department of Energy under contract number DE-AC02-76CH00016.

† Fritz-Haber-Institut, Faradayweg 4-6, D14195, Berlin, Germany.

‡ Department of Chemistry, University of Huddersfield, Huddersfield HD1 3DH, U.K.

References.

1. H. Ibach, J. Elect. Spectr. **64/65** 819 (1993).

2. G.P. Williams, Nucl. Instr. & Meth. **A291** 8 (1990).

3. C.J. Hirschmugl and G.P. Williams, Rev. Sci. Instr. **66**, 1487 (1995).

4. L.H. Yu, R. Biscardi, J. Bittner, E. Bozoki, J. Galayda, S. Krinsky, R. Nawrocky, O. Singh and G. Vignola, Proc. 1989 Particle Accelerator Conference, Chicago, IL, USA p. 1792 (1989).

5. C.J. Hirschmugl, Y.J. Chabal, F.M. Hoffmann, and G.P. Williams, J. Vac. Sci. Technol. **A12** 2229 (1994).

6. C.J. Hirschmugl, G.P. Williams, F.M. Hoffmann, and Y.J. Chabal, Phys. Rev. Lett. **65** 480 (1990).

7. C.L.A. Lamont, B.N.J. Persson and G.P. Williams, Chem. Phys. Letts. to be published.

8. B.N.J. Persson, Surface Science **269/270**, 103 (1992).

9. F. Wooten, *Optical Properties of Solids.* (Academic Press) 1972.

10. B.N.J. Persson, Phys. Rev. **B44** 3277 (1991).

11. B.N.J. Persson and A.I. Volokitin, Surface Science **310** 314 (1994).

12. B.N.J. Persson and A.I. Volokitin, Chem. Phys. Letts. **185** 292 (1991).

13. B.N.J. Persson, Chem. Phys. Letts. **197** 7 (1992).

14. B.N.J. Persson and A.I. Volokitin, Surface Science **310**, 314 (1994).

15. K. Lin, R.G. Tobin, P. Dumas, C.J.Hirschmugl and G.P. Williams, Phys. Rev. **B48** 2791 (1993).

16. P. Wissman, in Surface Physics - Springer Tracts in Modern Physics, ed. G. Höhler (Springer, Berlin) 1975.

17. C.J. Hirschmugl, G.P. Williams, B.N.J. Persson and A.I. Volokitin, Surface Science **317**, L1141 (1994).

18. B.E. Hayden, K. Prince, D.P. Woodruff, and A.M. Bradshaw, Physical Review Letters **51**, 475 (1983).

19. P. Hollins and J. Pritchard, Surface Science **89**, 486 (1979).

20. B.N.J. Persson and R.Ryberg, Physical Review **B24**, 6954 (1981).

21. C.J. Hirschmugl and G.P. Williams, Phys. Rev. B to be published.

Figure Captions.

Fig. 1. Absolute changes induced by CO overlayers on Cu surfaces. The inset shows the carbon-oxygen internal stretch. The carbon-metal vibration is the sharp dip at ~ 340 cm-1, the frustrated rotation is the peak at ~ 275 cm^{-1}. The heavy solid lines are the results of calculations based on Eq. 3.

Fig. 2. Absolute changes induced by a (3x3) overlayer of H on a Cu(111) surface. The smooth solid line is the results of calculations based on Eq. 3. The discrepancy at high frequencies is attributed to induced surface electronic states. The inset shows a theoretical anti-absorption resonance for a parallel vibrational mode from Eq. (3). The parameter $\alpha=(4n_aM\eta)/(cnm\cos\theta)$.

Fig. 3. The relative strengths of the normal and parallel electric field components at a metal surface for IRAS and EELS.

Fig. 4. The frequency-relaxation time diagram for Cu. Region A is the classical skin effect region, B, the relaxation region, C the transmission region, D the anomalous skin effect region and E the extreme anomalous skin effect region. The heavy solid line represents the region relevant to these experiments. The cartoons show schematically the electron trajectories near the surface.

Fig. 5. A comparison between the measured (dots) and theoretical (solid line) reflectance changes induced by a ($\sqrt{3}$ x $\sqrt{3}$) R30° CO overlayer on a Cu(111) surface, top panel, and a c(2 x 2) CO overlayer on a Cu(100) surface, bottom panel, and the calculation described in Ref. 17.

Fig. 6. Reflectivity spectra for various isotopic mixtures and concentrations of CO on Cu(100). The spectra (offset for clarity) are all ratioed with those from a clean Cu surface and thus represent adsorbate induced changes. The lower frequency peaks correspond to the frustrated rotational mode, while the dips are due to the carbon-metal bonding vibration. The dotted lines in the vicinity of the carbon-metal modes at ~ 340 cm^{-1} are the results obtained from a coherent potential approximation calculation. These latter do not have the background slope included.

Fig. 7. Frequencies measured for the frustrated rotational mode and carbon-metal bonding vibrational mode for a range of isotopic dilutions (▲ - upper axis) and coverages (▼ - lower axis) for CO/Cu(100). The data are linearly extrapolated to zero dilution and coverage.

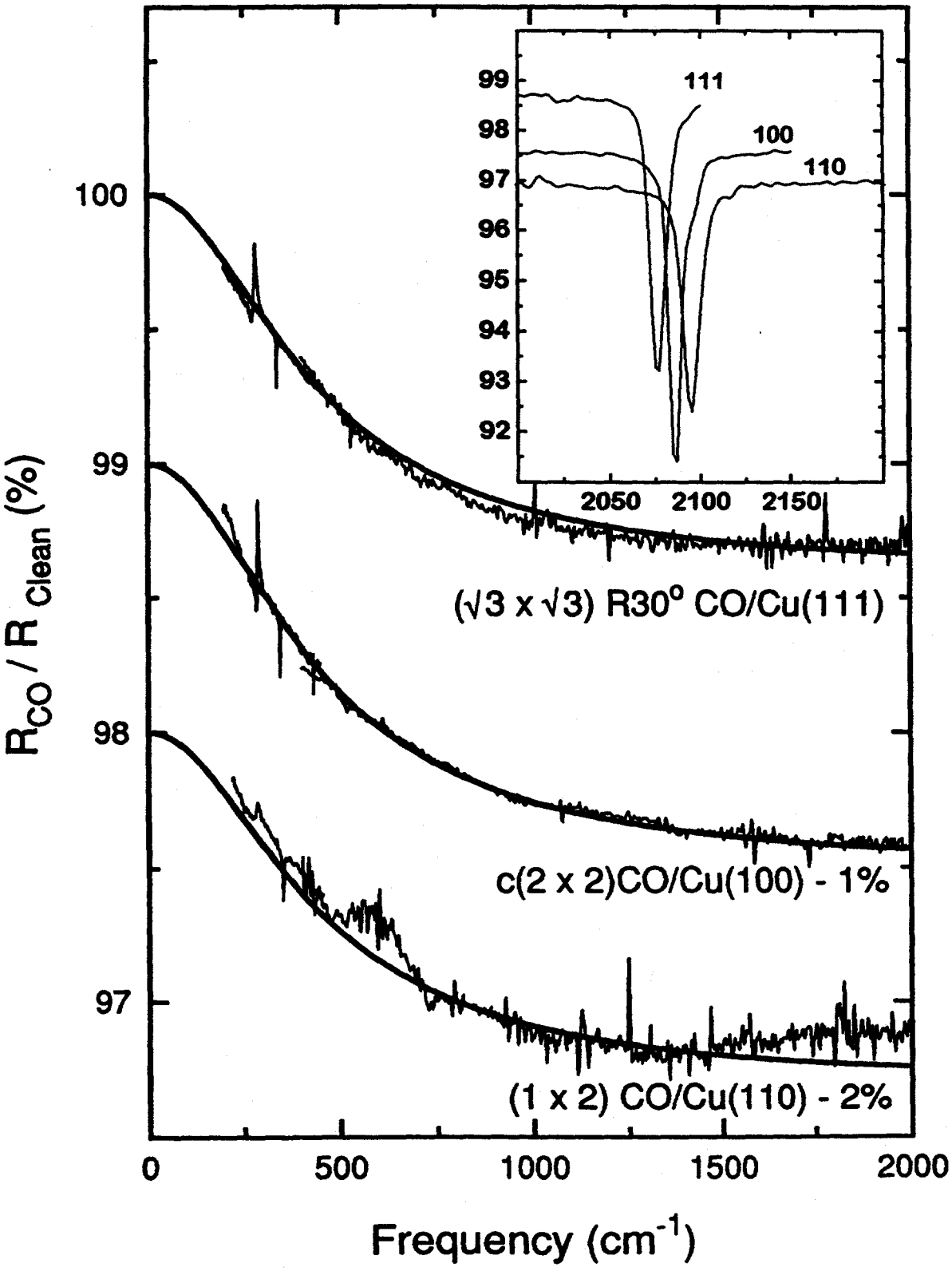

Hirschmugl, Lamont & Williams Fig. 1

9/28/95

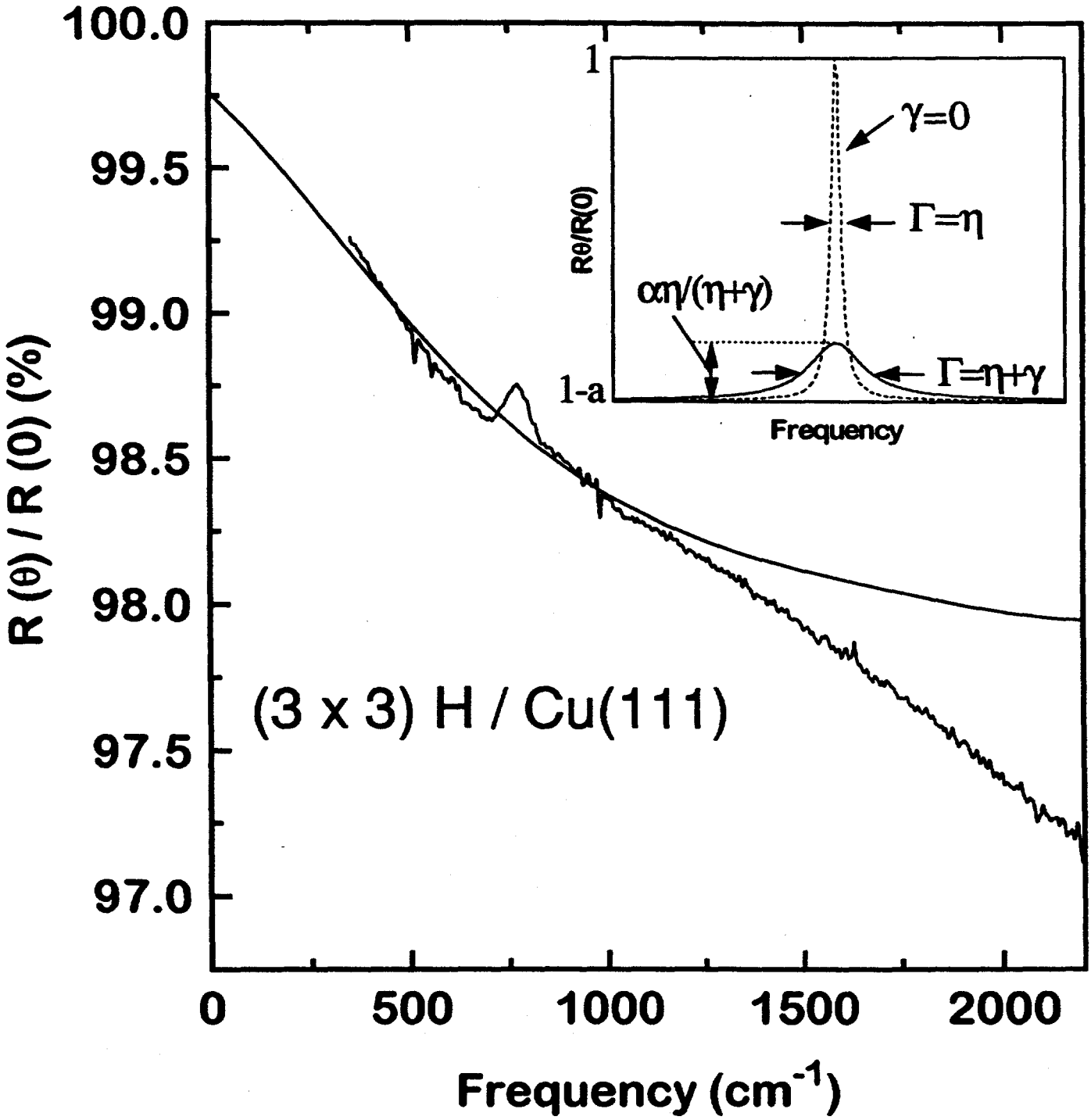

Hirschmugl, Lamont & Williams Fig. 2
9/28/95

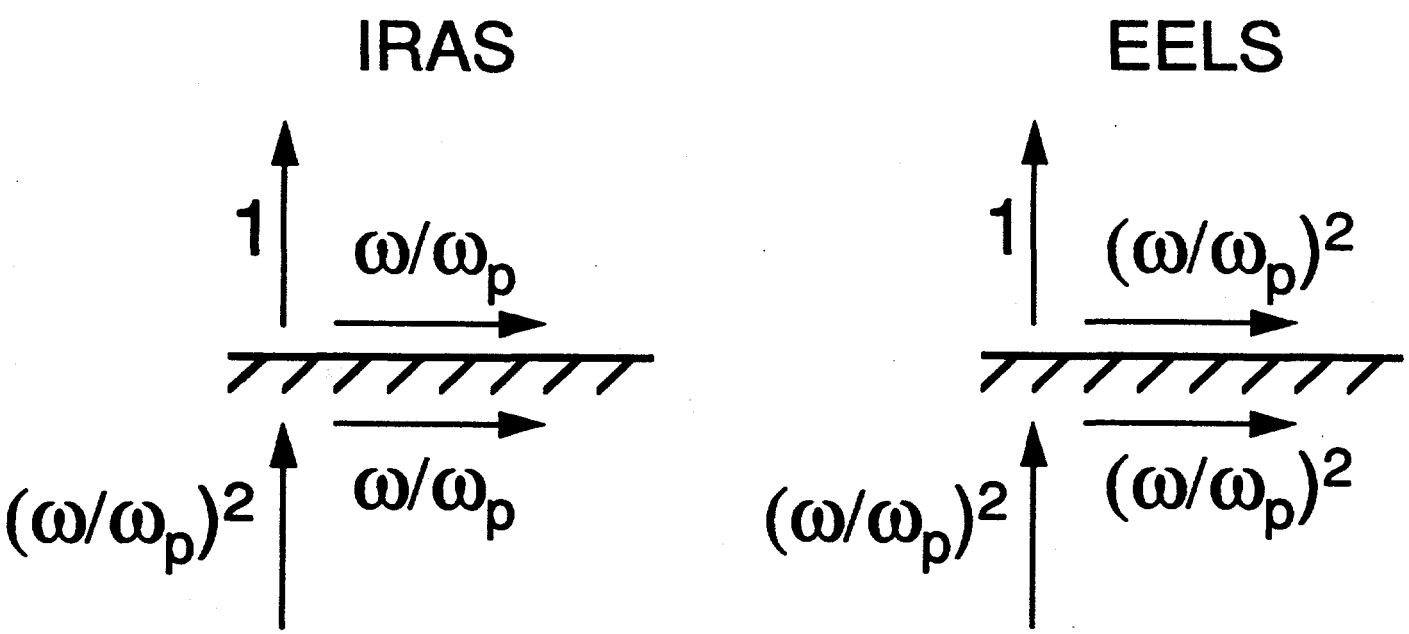
IRAS
1
ω/ω_p
$(\omega/\omega_p)^2$
ω/ω_p
EELS
1
$(\omega/\omega_p)^2$
$(\omega/\omega_p)^2$
$(\omega/\omega_p)^2$

FIG 3

D

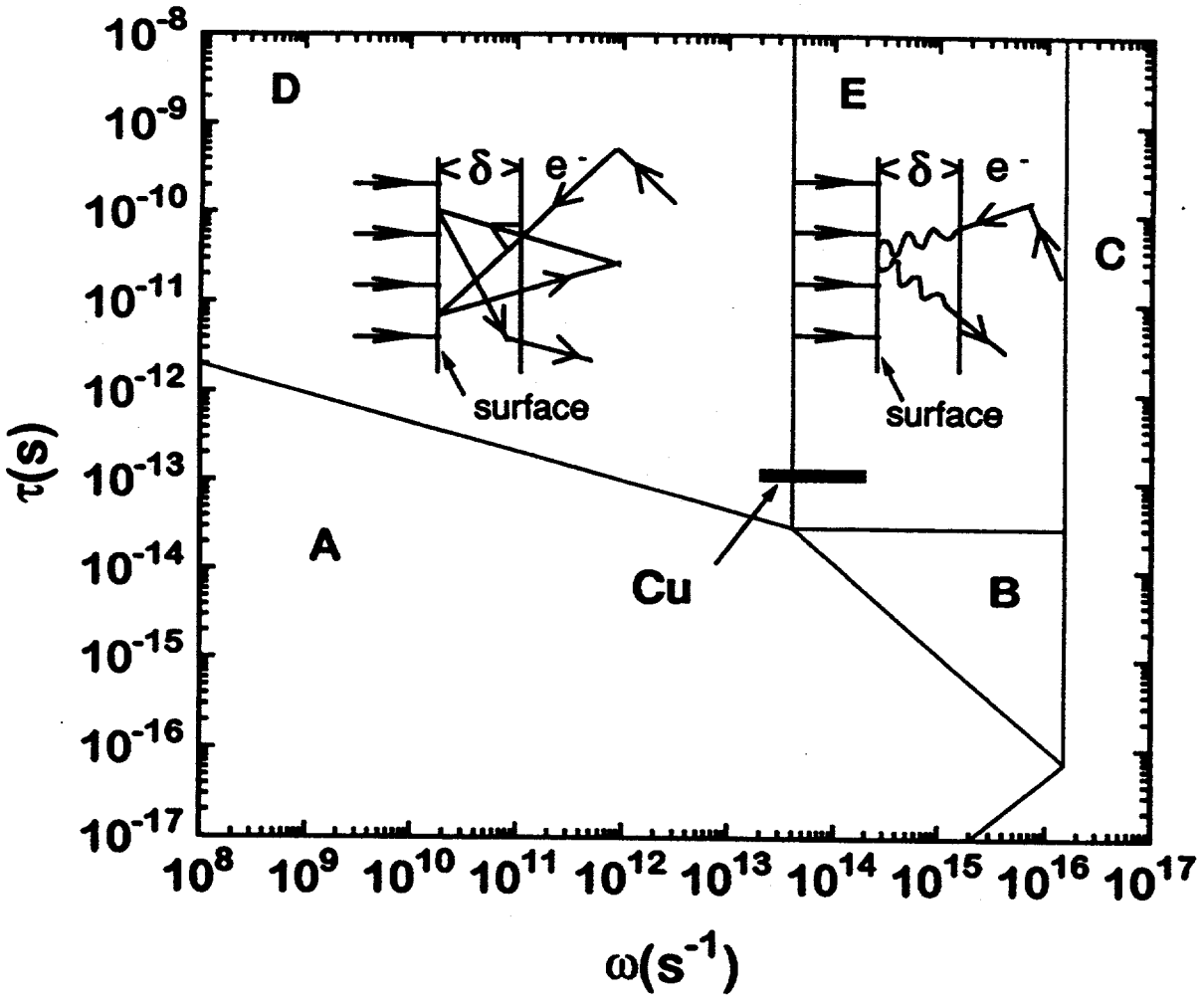
D
E
C
A
B
Cu
δ
e⁻
surface
δ
e⁻
surface
τ(s)
ω(s⁻¹)
10⁻⁸
10⁻⁹
10⁻¹⁰
10⁻¹¹
10⁻¹²
10⁻¹³
10⁻¹⁴
10⁻¹⁵
10⁻¹⁶
10⁻¹⁷
10⁸ 10⁹ 10¹⁰ 10¹¹ 10¹² 10¹³ 10¹⁴ 10¹⁵ 10¹⁶ 10¹⁷

FIG 4

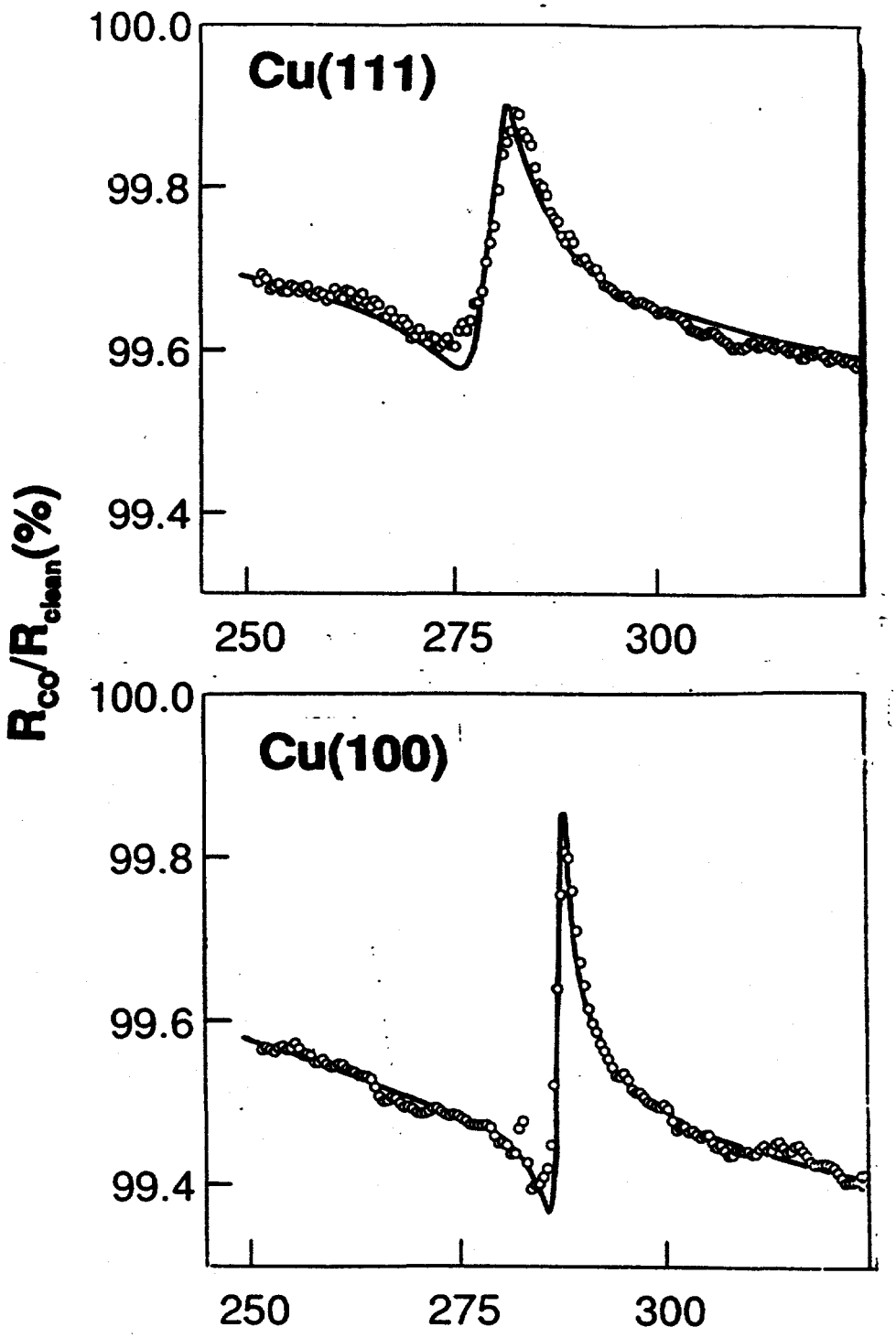
Cu(111)
100.0
99.8
99.6
99.4
250
275
300
Cu(100)
100.0
99.8
99.6
99.4
250
275
300
R_{co}/R_{clean}(%)

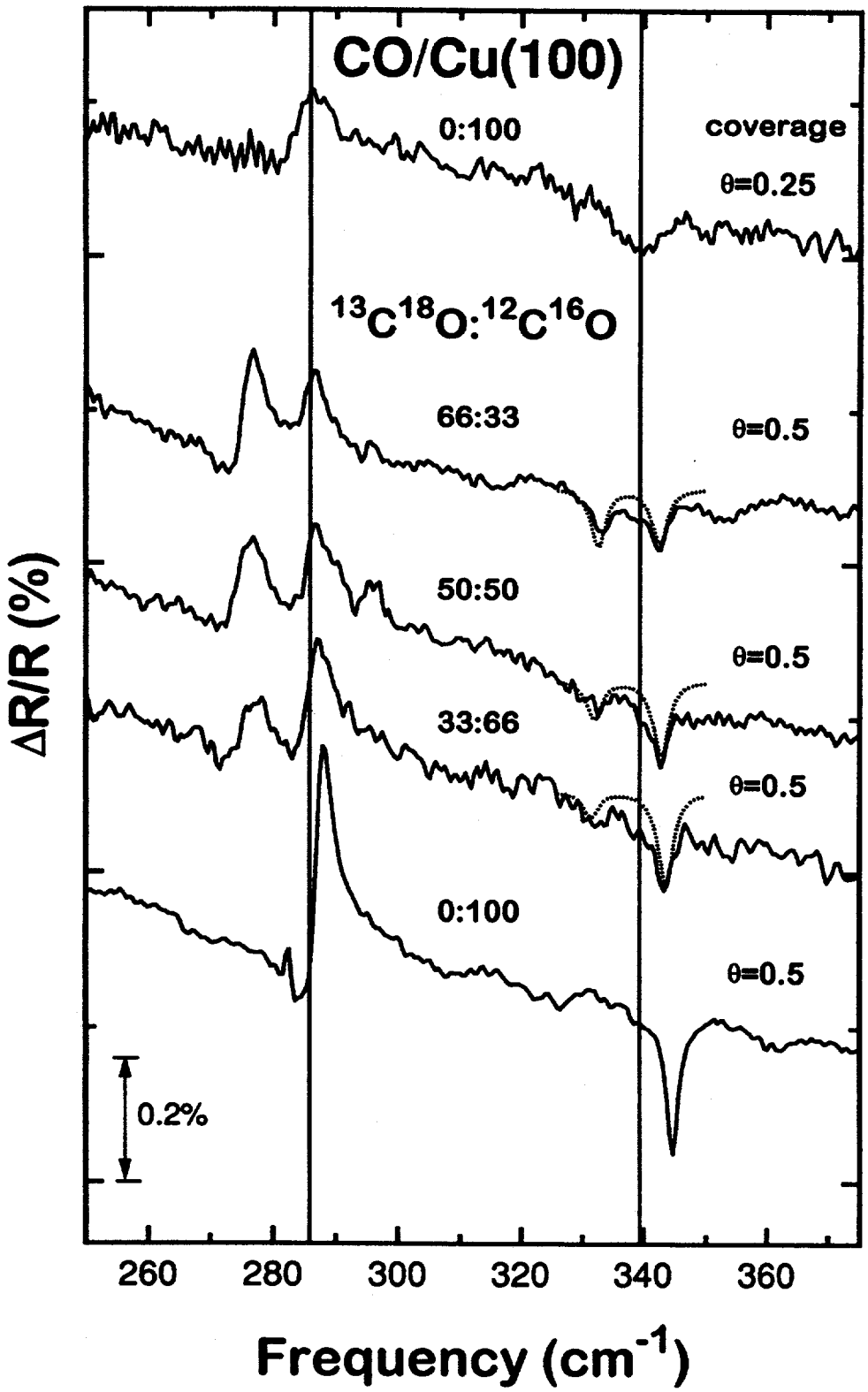

Hirschmugl, Lamont & Williams Fig. 6
9/28/95

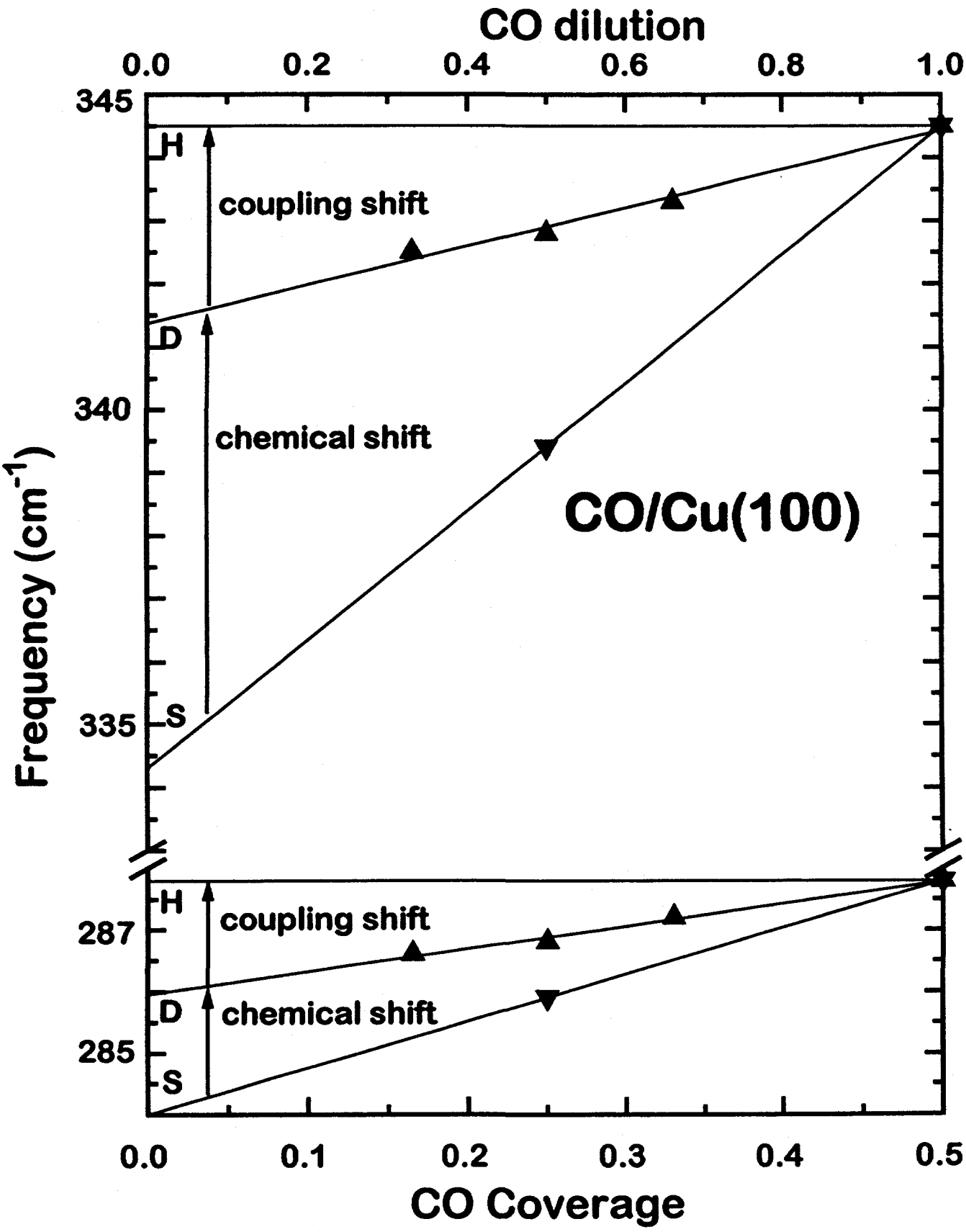

Hirschmugl, Lamont and Williams Fig.7
9/28/95